materials

MDPI

Article

High-Pressure Carbonation of Phosphogypsum for Calcium Carbonate Preparation and Crystal Modification Regulation

Shiyu Huang [1,2], Dongmei Liu [1,2,*], Xiaoxiang Zhang [1,2] and Taotao Zhang [3]

[1] College of Civil Engineering and Architecture, China Three Gorges University, Yichang 443002, China
[2] Hubei Key Laboratory of Disaster Prevention and Mitigation, Yichang 443002, China
[3] China Nuclear Industry Huaxing Construction Co., Nanjing 210019, China; 18306782903@163.com
* Correspondence: liudongmei@ctgu.edu.cn

Abstract

Phosphogypsum (PG) was used as a calcium source for preparing calcium carbonate ($CaCO_3$) through NH_4Cl leaching followed by high-pressure carbonation. The effects of NH_4Cl concentration, liquid-to-solid mass ratio, temperature, and leaching time on Ca^{2+} extraction were investigated, and the effects of CO_2 pressure, carbonation time, and $NH_3{\cdot}H_2O$ dosage on Ca^{2+} conversion were evaluated. The optimal conditions were an NH_4Cl concentration of 1.5 mol/L, a liquid-to-solid mass ratio of 60:1, a leaching temperature of 25 °C, a leaching time of 60 min, a CO_2 pressure of 1 MPa, a carbonation time of 10 min, and 12 vol% $NH_3{\cdot}H_2O$ addition. Under these conditions, the Ca^{2+} leaching rate and conversion rate reached 81.25% and 97.36%, respectively. The product obtained without organic additives was mainly spherical vaterite with partial particle agglomeration. Based on the optimized process, aspartic acid, glutamic acid, ethanol, and glycerol were introduced to regulate $CaCO_3$ crystallization. Appropriate additive dosages further improved Ca^{2+} conversion, promoted calcite as the dominant polymorph, and produced well-dispersed spherical $CaCO_3$ particles. Among the tested additives, glutamic acid and glycerol showed the strongest effects on crystal morphology regulation.

Keywords: phosphogypsum; high-pressure carbonation; NH_4Cl leaching; organic additives; calcium carbonate

1. Introduction

Phosphogypsum (PG), a solid waste by-product generated by the wet-process phosphoric acid industry, is produced in large quantities annually in Yichang, Province, China, a major phosphate-resource region in the Yangtze River Basin [1,2]. In the context of China's "Dual Carbon" goals, namely carbon peaking and carbon neutrality, the conversion of PG into calcium carbonate ($CaCO_3$) through carbonation offers a promising strategy for both CO_2 utilization and solid-waste valorization [3,4]. However, the practical utilization of PG for $CaCO_3$ preparation depends largely on developing a simple, low-cost, and efficient route for extracting calcium from the gypsum phase.

$CaCO_3$ exists in three major polymorphs, among which calcite is the thermodynamically stable phase under ambient conditions [5,6]. Carbonation processes are generally classified into direct and indirect routes. Direct carbonation is suitable for calcium-rich systems containing a high content of free calcium oxide (f-CaO). Because calcium in PG mainly exists as calcium sulfate, an indirect carbonation route was adopted in this study to facilitate calcium extraction and subsequent control of $CaCO_3$ precipitation. It should be

Check for updates

Received: 21 May 2026
Revised: 16 June 2026
Accepted: 16 June 2026
Published: 1 July 2026

Copyright: © 2026 by the authors. Licensee MDPI, Basel, Switzerland. This article is an open access article distributed under the terms and conditions of the Creative Commons Attribution (CC BY) license.

noted that direct carbonation of calcium sulfate has also been reported to be feasible, even at room temperature [7]. Previous studies [8–11] have commonly employed strong acid or alkali leaching for calcium recovery; however, these approaches may cause severe equipment corrosion and co-dissolution of impurities. In comparison, NH_4Cl is a low-cost and widely available salt leaching agent. During NH_4Cl leaching, $CaSO_4 \cdot 2H_2O$, the dominant gypsum phase in PG, partially dissolves and releases Ca^{2+} into the leachate [12]. Qiao et al. and Chen et al. [13,14] independently used NH_4Cl solutions to leach PG and subsequently prepared $CaCO_3$ by bubbling CO_2 into the Ca^{2+}-rich leachate, achieving Ca^{2+} conversion rates of approximately 80%. The resulting products were predominantly vaterite, characterized by spherical particles and fine, loose $CaCO_3$ aggregates on their surfaces, with noticeable agglomeration. After Ca^{2+} leaching in the indirect process, the subsequent carbonation stage using conventional CO_2 bubbling is limited by the low solubility of CO_2 and slow gas–liquid mass transfer, resulting in slow reaction kinetics, prolonged carbonation times, and relatively low Ca^{2+} conversion efficiencies. High-pressure carbonation can effectively alleviate these limitations. López-Periago et al. [15] carbonated a $Ca(OH)_2$ suspension under ultrasonic stirring at 40 °C and 13 MPa for 10 min, achieving a Ca^{2+} conversion rate of 88%. The obtained $CaCO_3$ was calcite with a rhombic morphology formed through polycrystalline aggregation.

Previous studies have mainly focused on optimizing leaching and carbonation conditions and have shown that $CaCO_3$ polymorphs and morphologies can be regulated either by adjusting carbonation parameters or by introducing additives. Nevertheless, the regulation of $CaCO_3$ polymorphs and morphologies in PG-derived calcium leachate systems, particularly under high-pressure carbonation conditions, remains insufficiently understood. Seo et al. [16] investigated the effect of ethanol concentration on $CaCO_3$ formation by adding different amounts of ethanol to a $Ca(OH)_2$ solution prior to CO_2 bubbling. They found that increasing ethanol concentration gradually decreased the average particle size of the resulting $CaCO_3$ and shifted the dominant polymorph from calcite to vaterite. Jin et al. [17] conducted carbonation in a $Ca(OH)_2$–ethanol system at 40 °C, 10 MPa, and 600 rpm for 2 h. The products were mainly vaterite, appearing as porous microspheres with uniform morphologies and no obvious agglomeration. Konopacka-Łyskawa et al. [18] performed CO_2 bubbling carbonation in a $Ca(OH)_2$ system containing 0–20% ethanol or glycerol at 20 °C and 900 rpm. Pure calcite was obtained under all tested conditions. Without additives, the $CaCO_3$ particles had an average size of 9 μm. As the organic solvent concentration increased, the solution viscosity increased, leading to a gradual reduction in particle size; in particular, the 20% glycerol system produced particles with a size distribution of 0.1–0.59 μm. Luo et al. [19] introduced aspartic acid solutions at different concentrations into $Ca(OH)_2$ suspensions and prepared $CaCO_3$ by CO_2 carbonation, obtaining products dominated by vaterite. Yang et al. [20] prepared $CaCO_3$ by mixing $Ca(OH)_2$ powder with 0–10% aspartic acid or glutamic acid solutions, followed by CO_2 aeration at 20 °C for 2 h. In the absence of amino acids, pure calcite with a particle size of 1–2 μm was obtained. Aspartic acid and glutamic acid can selectively adsorb onto specific crystal faces of thermodynamically stable calcite [20,21], thereby inhibiting its preferential growth. As a result, the dominant polymorph shifted to vaterite after amino acid addition, and the particle size decreased. These studies indicate that additives can significantly affect $CaCO_3$ crystallization. Alcohols can regulate solution viscosity, stabilize the calcite phase, and control particle size [15–17]. In contrast, amino acids can coordinate with Ca^{2+} through their carboxyl groups during the prenucleation stage, thereby affecting the formation and stability of calcium-containing precursor species. In addition, their selective adsorption on specific calcite facets can inhibit the preferential growth of calcite, which may favor the retention of metastable vaterite. However, most of these conclusions were derived from

atmospheric-pressure bubbling carbonation experiments using $Ca(OH)_2$ as the calcium source [18,19]. This system differs substantially from the PG-derived calcium leachate system under high-pressure carbonation used in the present study. Therefore, the corresponding polymorph and morphology regulation mechanisms require further clarification.

NH_4Cl was selected as the leaching agent because of its low cost, wide availability, and mild leaching conditions. During NH_4Cl leaching, $CaSO_4 \cdot 2H_2O$ in PG partially dissolves, releasing Ca^{2+} and SO_4^{2-} into the NH_4Cl-containing leachate. The filter cake mainly consists of undissolved PG residues and less soluble impurity phases, while minor amounts of soluble impurity species may also enter the leachate. Therefore, the main objective of this study was to develop a simple and cost-effective route for extracting Ca^{2+} from PG and converting it into $CaCO_3$ through high-pressure carbonation. First, the effects of the liquid-to-solid mass ratio, NH_4Cl concentration, reaction temperature, and leaching time on the Ca^{2+} leaching rate were investigated. Subsequently, the effects of CO_2 pressure, carbonation time, and $NH_3 \cdot H_2O$ addition on the Ca^{2+} conversion rate were examined to optimize the carbonation process. Finally, aspartic acid, glutamic acid, ethanol, and glycerol were introduced to evaluate their effects on the Ca^{2+} conversion rate, $CaCO_3$ polymorphs, and microscopic morphologies.

2. Materials and Methods

2.1. Materials

PG samples were collected from a phosphogypsum stockpile in Yichang, Hubei Province, China, and appeared as a grayish-brown solid. Before use, the samples were dried at 100 °C to constant mass, pulverized using a ball mill, and passed through a 0.15 mm sieve to obtain the pretreated feedstock.

The chemical composition, microstructure, and X-ray diffraction (XRD) pattern of the raw PG are shown in Table 1, Figure 1, and Figure 2, respectively. All chemical reagents used in this study were of analytical grade unless otherwise stated. Ammonium chloride (NH_4Cl, analytical grade, Sinopharm Chemical Reagent Co., Ltd., Shanghai, China), ammonia solution ($NH_3 \cdot H_2O$, concentration or purity, Sinopharm Chemical Reagent Co., Ltd., Shanghai, China), ethanol (C_2H_5OH, analytical grade, Sinopharm Chemical Reagent Co., Ltd., Shanghai, China), and glycerol ($C_3H_8O_3$, analytical grade, Sinopharm Chemical Reagent Co., Ltd., Shanghai, China) were used. Aspartic acid ($C_4H_7NO_4$, analytical grade, Shanghai Macklin Biochemical Co., Ltd., Shanghai, China) and glutamic acid ($C_5H_9NO_4$, analytical grade, Shanghai Macklin Biochemical Co., Ltd., Shanghai, China) were also used.

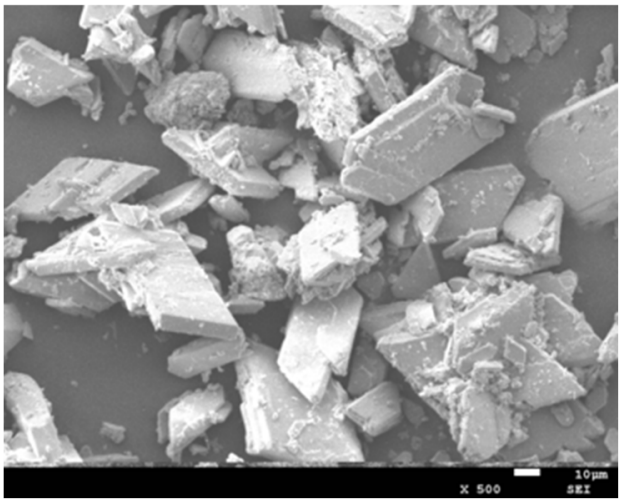

Figure 1. SEM image of raw PG.

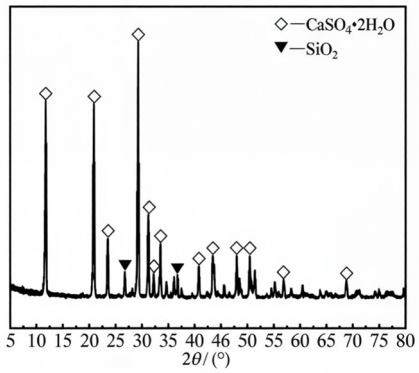

Figure 2. XRD pattern of raw PG. Symbols: ◇, $CaSO_4 \cdot 2H_2O$; ▼, SiO_2.

Table 1. Chemical composition of raw PG (wt%).

SO_3	CaO	SiO_2	$A1_2O_3$	Fe_2O_3	K_2O	CuO	P_2O_5	F	Loss
50.22	35.31	10.94	0.57	0.68	0.56	0.02	0.59	0.87	0.24

2.2. Preparation of $CaCO_3$

Leaching of Ca^{2+} from PG

Using a one-factor approach, 5 g of PG was added to NH_4Cl solutions with different concentrations of 0.1–2.0 mol/L to prepare suspensions with liquid-to-solid mass ratios of 10:1–60:1. The suspensions were reacted at different temperatures of 25–85 °C for 10–120 min. After leaching, vacuum filtration was performed for solid–liquid separation. The filtrate was collected as the Ca^{2+}-rich leachate, while the filter cake mainly consisted of undissolved PG residues and less soluble impurity phases.

Before carbonation, $NH_3 \cdot H_2O$ solution was added to the Ca^{2+}-rich leachate at different dosages of 4–16 vol%. The mixture was then transferred into a high-pressure reactor for carbonation. The carbonation reaction was conducted at 25 °C using CO_2 with a purity of 99 vol% under pressures of 0.1–2.0 MPa for 4–15 min. After the reaction, the slurry was allowed to stand at room temperature for 2 h. The $CaCO_3$ solids were then separated using a 0.1 μm membrane filter, thoroughly washed with deionized water, and dried at 80 °C to constant mass.

Aspartic acid, glutamic acid, ethanol, and glycerol were separately introduced into the Ca^{2+}-rich leachate. The mixtures were carbonated for 10 min under the optimized conditions of 12 vol% $NH_3 \cdot H_2O$ addition, 25 °C, and a CO_2 pressure of 1.0 MPa. After carbonation, the slurry was filtered using a 0.1 μm membrane filter to collect the $CaCO_3$ solids. The collected solids were thoroughly washed with deionized water and dried at 80 °C to constant mass.

2.3. Experimental Methods and Characterization

2.3.1. Determination of Ca^{2+} Leaching Rate

The Ca^{2+} leaching rate reported in this study represents the experimentally measured apparent recovery of calcium from PG, rather than a theoretical equilibrium solubility value. First, 25 mL of the Ca^{2+}-rich leachate was diluted tenfold with deionized water. Then, 25 mL of the diluted solution was collected, and the Ca^{2+} concentration was determined by EDTA titration. The amount of Ca^{2+} in the leachate, denoted as n_2, was calculated from the volume of EDTA consumed. Finally, the Ca^{2+} leaching rate, η, was calculated using Equation (1):

$$\eta = \frac{n_2}{n_1} \times 100\% \quad (1)$$

where n_1 is the amount of Ca^{2+} in $CaSO_4 \cdot 2H_2O$ in PG (mol), and n_2 is the amount of Ca^{2+} in the leaching solution (mol).

2.3.2. Determination of Ca^{2+} Conversion Rate

After carbonation, the slurry was allowed to stand for 2 h and then filtered through a 0.05 μm membrane filter. The residual Ca^{2+} concentration in the filtrate was determined by EDTA titration, and the amount of residual Ca^{2+}, denoted as n_3, was calculated from the volume of EDTA consumed. The Ca^{2+} conversion rate, α, was then calculated using Equation (2):

$$\alpha = \frac{n_2 - n_3}{n_2} \times 100\% \quad (2)$$

where n_2 is the amount of Ca^{2+} in the leaching solution (mol), and n_3 is the amount of Ca^{2+} in the filtrate after carbonation (mol).

2.3.3. Characterization Methods

The composition of PG and $CaCO_3$ was qualitatively identified by X-Ray diffraction (XRD) using a SmartLab (9 kW) diffractometer (Rigaku Corporation, Tokyo, Japan). The morphology of PG and $CaCO_3$ was observed using a 3200A scanning electron microscope (SEM) (Gwqnt Quantum, Hefei, China) operated at an accelerating voltage of 0.2–30 kV.

3. Results and Discussion

3.1. Process for $CaCO_3$ Preparation via High-Pressure Carbonation of Phosphogypsum

3.1.1. Leaching Rate of Ca^{2+} in PG

Figure 3 shows the effects of the liquid-to-solid mass ratio, NH_4Cl concentration, reaction temperature, and reaction time on the Ca^{2+} leaching rate.

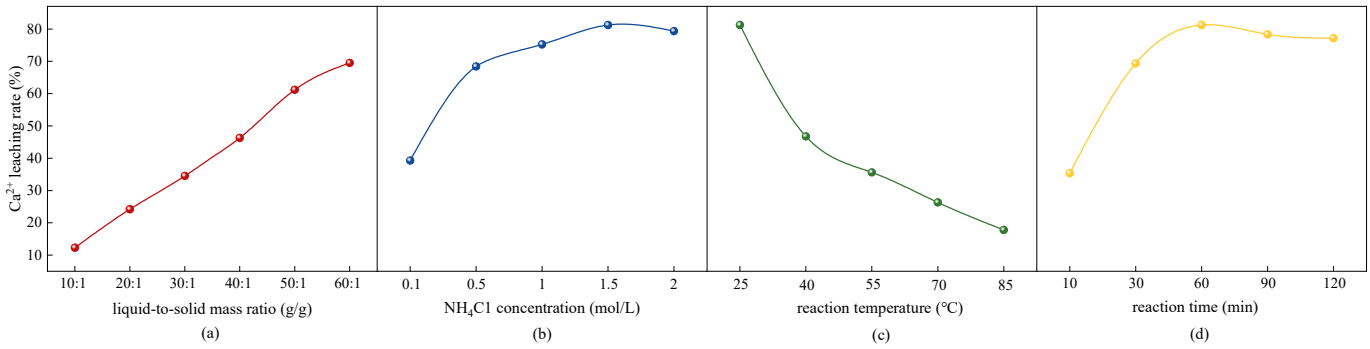

Figure 3. Effects of (**a**) liquid-to-solid mass ratio, (**b**) NH_4Cl concentration, (**c**) reaction temperature, and (**d**) reaction time on the Ca^{2+} leaching rate.

After reaction with 0.5 mol/L NH_4Cl at 25 °C for 60 min, the Ca^{2+} leaching rate increased markedly with increasing liquid-to-solid mass ratio. The maximum leaching rate of 69.5% was obtained at a liquid-to-solid mass ratio of 60:1. NH_4Cl can hydrolyze in water to release H^+, thereby lowering the solution pH [22]. As the liquid-to-solid mass ratio increased, the amount of NH_4Cl solution available per unit mass of PG increased, which provided more favorable conditions for the dissolution of $CaSO_4 \cdot 2H_2O$. In addition, the increased solution volume reduced the accumulation of dissolved Ca^{2+} and SO_4^{2-} near the solid surface, thereby promoting mass transfer and facilitating further dissolution of the gypsum phase. These effects contributed to the increase in the Ca^{2+} leaching rate.

At 25 °C, with a liquid-to-solid mass ratio of 60:1 and a reaction time of 60 min, the Ca^{2+} leaching rate first increased significantly and then decreased slightly with increasing NH_4Cl concentration. The maximum leaching rate of 81.25% was achieved at an NH_4Cl

concentration of 1.5 mol/L. With increasing NH_4Cl concentration, the ionic strength of the leaching solution increased, and ion interactions such as Ca^{2+}–Cl^- association became more pronounced. These effects can reduce the effective concentration of free Ca^{2+} in solution and shift the dissolution equilibrium of $CaSO_4 \cdot 2H_2O$ toward further dissolution, thereby increasing the Ca^{2+} leaching rate. However, when the NH_4Cl concentration was further increased to 2.0 mol/L, the excessive ion concentration increased the solution viscosity [22], which hindered the diffusion of Ca^{2+} and SO_4^{2-} and led to a slight decrease in the Ca^{2+} leaching rate.

At a liquid-to-solid mass ratio of 60:1 and an NH_4Cl concentration of 1.5 mol/L, the Ca^{2+} leaching rate decreased with increasing reaction temperature after 60 min of leaching. The maximum leaching rate of 81.25% was obtained at 25 °C. This decreasing trend may be attributed to the reduced solubility of PG at elevated temperatures [23], which lowers the concentration of dissolved Ca^{2+} in the leaching solution and consequently decreases the Ca^{2+} leaching rate.

At 25 °C, with an NH_4Cl concentration of 1.5 mol/L and a liquid-to-solid mass ratio of 60:1, the Ca^{2+} leaching rate initially increased and then tended to stabilize with increasing reaction time. The maximum leaching rate of 81.25% was achieved at 60 min. Sufficient reaction time is required for NH_4Cl diffusion and its interaction with PG particles. Therefore, extending the leaching time promotes more complete calcium extraction and increases the Ca^{2+} leaching rate. However, excessive leaching time may lead to local supersaturation of Ca^{2+} and SO_4^{2-}, thereby promoting the reprecipitation of $CaSO_4$. In addition, trace Fe^{3+} in PG may gradually dissolve during prolonged leaching and interact with SO_4^{2-} to form hydrated ferric sulfate species, such as $Fe_2(SO_4)_3 \cdot xH_2O$ [24]. These processes may reduce the amount of dissolved calcium remaining in solution, resulting in a slight decrease in the Ca^{2+} leaching rate.

In summary, the optimal conditions for Ca^{2+} extraction from PG using NH_4Cl leaching were determined to be a reaction temperature of 25 °C, an NH_4Cl concentration of 1.5 mol/L, a liquid-to-solid mass ratio of 60:1, and a leaching time of 60 min.

3.1.2. Conversion Rate of Ca^{2+} in the Leaching Solution

Figure 4 shows the Ca^{2+} conversion rate as a function of CO_2 pressure, carbonation time, and $NH_3 \cdot H_2O$ addition at 25 °C.

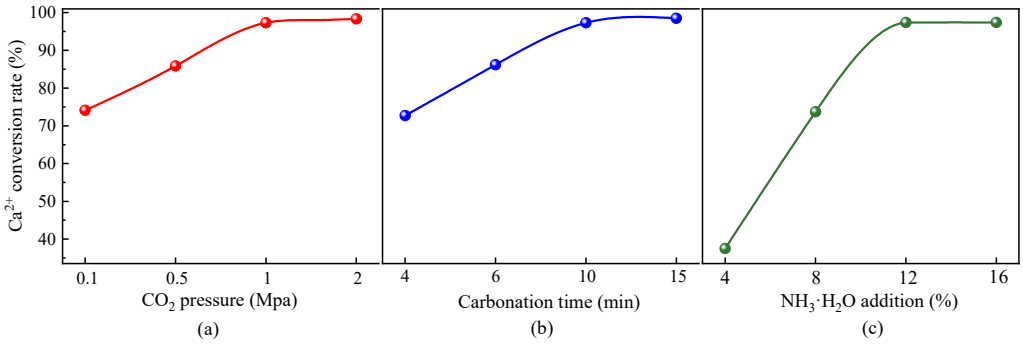

Figure 4. Effects of (**a**) CO_2 pressure, (**b**) carbonation time, and (**c**) $NH_3 \cdot H_2O$ addition on the Ca^{2+} conversion rate at 25 °C.

Under the conditions of 12 vol% $NH_3 \cdot H_2O$ addition and a carbonation time of 10 min, the Ca^{2+} conversion rate increased markedly as the CO_2 pressure increased from 0.1 to 1.0 MPa. However, when the pressure was further increased to 2.0 MPa, the additional improvement was limited, with the conversion rate reaching 98.34%. Compared with previous studies [12–14] using CO_2 bubbling at atmospheric pressure, the present high-

pressure carbonation process achieved a higher Ca^{2+} conversion rate within a shorter reaction time and under milder temperature conditions. In a sealed reactor, according to the ideal gas law, increasing the CO_2 pressure at a constant temperature increases the amount of CO_2 per unit volume. The higher CO_2 concentration provides a stronger driving force for gas–liquid mass transfer [25], thereby promoting CO_2 diffusion into the bulk liquid. In addition, according to Henry's law, increasing the pressure enhances the solubility of CO_2 in the solution. Dissolved CO_2 reacts with water and undergoes stepwise dissociation to form carbonate species. Under alkaline conditions provided by $NH_3 \cdot H_2O$, the concentration of CO_3^{2-} increases, which promotes its reaction with Ca^{2+} to form $CaCO_3$ precipitates and thus increases the Ca^{2+} conversion rate. However, excessive CO_2 dissolution at higher pressure may generate more carbonic acid and lower the system pH, shifting the carbonate equilibrium toward HCO_3^-. This may favor the formation of soluble calcium bicarbonate species and limit the further increase in the Ca^{2+} conversion rate.

Under the conditions of 12 vol% $NH_3 \cdot H_2O$ addition and a CO_2 pressure of 1.0 MPa, the Ca^{2+} conversion rate increased rapidly as the carbonation time was extended from 4 to 10 min. When the carbonation time was further extended to 15 min, the additional increase was limited, with the conversion rate ultimately reaching 98.51%. During the initial stage of carbonation, the Ca^{2+} concentration in the leachate was high, and the carbonate species generated from dissolved CO_2 rapidly reacted with Ca^{2+} to form $CaCO_3$ precipitates. At this stage, the reactant concentrations were relatively high, the diffusion distance was short, and the mass-transfer resistance was low, resulting in a rapid increase in the Ca^{2+} conversion rate. As carbonation proceeded, Ca^{2+} in the solution was progressively consumed, leading to a decrease in ion concentration and a reduced driving force for precipitation. Therefore, the increase in the Ca^{2+} conversion rate gradually slowed at longer carbonation times.

After carbonation for 10 min at a CO_2 pressure of 1.0 MPa, the Ca^{2+} conversion rate initially increased substantially and then plateaued with increasing $NH_3 \cdot H_2O$ addition. A Ca^{2+} conversion rate of 97.36% was achieved at 12 vol% $NH_3 \cdot H_2O$ addition. As the $NH_3 \cdot H_2O$ concentration increased, dissolved CO_2 reacted with $NH_3 \cdot H_2O$ to form ammonium carbonate species, which subsequently dissociated to provide CO_3^{2-}. Meanwhile, the increased $NH_3 \cdot H_2O$ addition maintained an alkaline environment, promoting the conversion of dissolved CO_2 into carbonate species. The resulting increase in CO_3^{2-} concentration allowed more Ca^{2+} to precipitate as $CaCO_3$, thereby increasing the Ca^{2+} conversion rate. However, at 16 vol% $NH_3 \cdot H_2O$ addition, most of the Ca^{2+} had already precipitated as $CaCO_3$, and the formed $CaCO_3$ particles increased the mass-transfer resistance for the remaining unreacted Ca^{2+} and CO_3^{2-}. Consequently, the Ca^{2+} conversion rate showed little further increase. Therefore, 12 vol% $NH_3 \cdot H_2O$ addition was selected as the optimal dosage because it enabled efficient Ca^{2+} conversion while avoiding reagent waste and the undesirable particle-size increase associated with excessive $NH_3 \cdot H_2O$ addition [26].

In summary, a Ca^{2+} conversion rate of 97.36% was achieved under the optimized carbonation conditions: 12 vol% $NH_3 \cdot H_2O$ addition, a carbonation temperature of 25 °C, a CO_2 pressure of 1.0 MPa, and a carbonation time of 10 min.

3.1.3. Crystal Morphology Under Optimal High-Pressure Carbonation Conditions

Figures 5 and 6 show the SEM image and XRD pattern of calcium carbonate prepared from PG under the optimized high-pressure carbonation conditions, respectively. The obtained $CaCO_3$ crystals were predominantly spherical, and band-like aggregates formed by the assembly of spherical particles were also observed. The XRD results indicated that the product was mainly composed of vaterite, with only trace amounts of calcite. In

addition, the product contained a relatively high proportion of large particles, whereas fine particles were less developed.

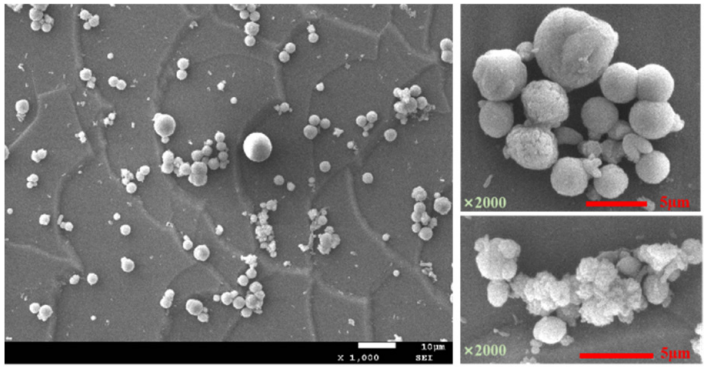

Figure 5. SEM images of $CaCO_3$ under the optimized high-pressure carbonation conditions.

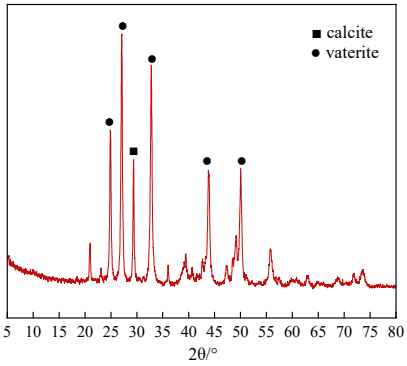

Figure 6. XRD pattern of $CaCO_3$ under the optimized high-pressure carbonation conditions.

In the aqueous carbonation system, NH_4^+ may interact with the hydrated surfaces of $CaCO_3$ crystallites, thereby affecting particle aggregation and crystal growth. The adsorption of NH_4^+ may alter the surface interactions among $CaCO_3$ particles, leading to crystal agglomeration, and may also modify the growth rates of specific crystal faces. These effects can change the crystal growth direction and contribute to the formation of the branched structures observed in the product [22]. In addition, NH_4^+ may adsorb onto active sites on calcite surfaces, such as the {104} facet, thereby blocking growth sites and inhibiting calcite development. According to the Ostwald ripening process, metastable vaterite can gradually transform into thermodynamically stable calcite with prolonged reaction time [5]. This transformation may partially offset the inhibitory effect of NH_4^+ on calcite growth, which explains the presence of weak calcite diffraction peaks in the XRD pattern.

3.2. Modulation of $CaCO_3$ Polymorphs via Organic Additives

The $CaCO_3$ crystals prepared under the optimized high-pressure carbonation conditions were predominantly vaterite; however, particle agglomeration and a non-uniform size distribution were observed. As a metastable $CaCO_3$ polymorph with relatively low thermodynamic stability and crystallinity [5,6], vaterite is prone to phase transformation during storage or application, which may lead to performance degradation. Therefore, organic additives were introduced before carbonation of the Ca^{2+}-rich leachate to regulate $CaCO_3$ crystallization and improve the morphological uniformity of the products. In this study, the effects of these additives on the Ca^{2+} conversion rate, polymorph composition, and crystal morphology of the resulting $CaCO_3$ were investigated.

3.2.1. Ca^{2+} Conversion Rate in Leachate with Different Organic Additives

Figure 7 shows the effect of additive concentration on the Ca^{2+} conversion rate.

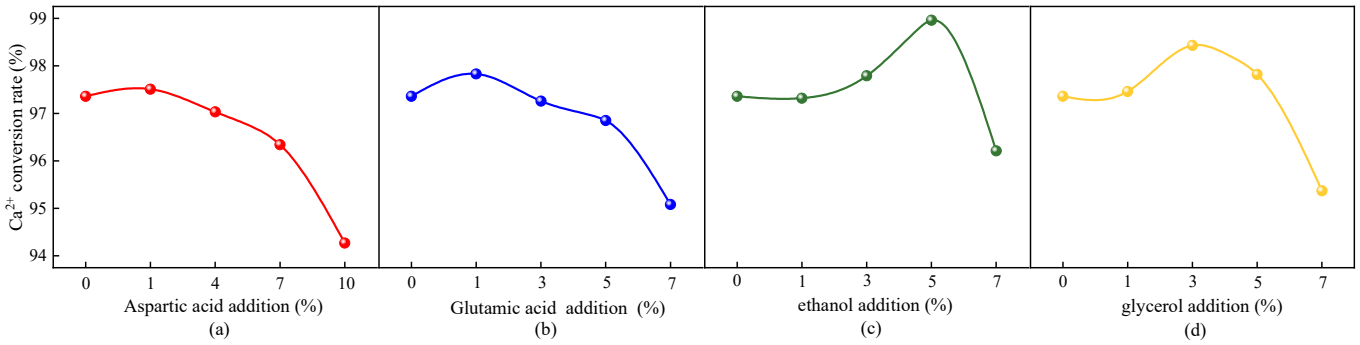

Figure 7. Effects of different organic additives on the Ca^{2+} conversion rate: (**a**) aspartic acid, (**b**) glutamic acid, (**c**) ethanol, and (**d**) glycerol.

With increasing aspartic acid and glutamic acid concentrations, the Ca^{2+} conversion rate initially increased slightly and then decreased. The maximum conversion rates of 97.51% and 97.83% were achieved at 1 wt% aspartic acid and 1 wt% glutamic acid, respectively. Aspartic acid and glutamic acid can provide nucleation sites for $CaCO_3$ formation [27]. Therefore, at low concentrations, these additives promote $CaCO_3$ nucleation and slightly enhance the Ca^{2+} conversion rate. However, when their concentrations exceed a certain threshold, steric hindrance may occur [27], which hinders the diffusion of Ca^{2+} and CO_3^{2-} toward the growing crystal surfaces. In addition, aspartic acid and glutamic acid can form stable complexes with Ca^{2+} [20,27,28], thereby reducing the concentration of free Ca^{2+} in solution. According to the solubility product relationship of $CaCO_3$, $Ksp = [Ca^{2+}][CO_3^{2-}]$, a decrease in free Ca^{2+} requires a higher CO_3^{2-} concentration to initiate precipitation. This increases the precipitation barrier, inhibits $CaCO_3$ formation, and ultimately leads to a decrease in the Ca^{2+} conversion rate.

The Ca^{2+} conversion rate also showed an initial increase followed by a decrease with increasing ethanol and glycerol concentrations. The maximum conversion rates of 98.96% and 98.43% were obtained at 5% ethanol and 3% glycerol, respectively. At low additive concentrations, both alcohols can increase solution supersaturation and reduce the nucleation barrier, thereby accelerating the early-stage nucleation of $CaCO_3$ [29–31]. This promotes the reaction between Ca^{2+} and CO_3^{2-}, resulting in a slight increase in the Ca^{2+} conversion rate. However, as the alcohol concentration further increases, excessive alcohols significantly increase the solution viscosity [16,18]. The increased viscosity reduces the diffusion coefficients of Ca^{2+} and CO_3^{2-} and slows their transport in the solution. Consequently, these ions cannot diffuse to the crystal growth sites in time, which retards the growth of $CaCO_3$ nuclei. The abundant nuclei formed at the initial stage cannot obtain sufficient reactants for continuous growth, eventually leading to a decrease in the Ca^{2+} conversion rate.

3.2.2. Crystal Morphology of $CaCO_3$ with Different Organic Additives

Figures 8 and 9 show the SEM images and XRD patterns of $CaCO_3$ prepared in the presence of different organic additives, respectively. With the addition of aspartic acid, glutamic acid, ethanol, or glycerol, calcite became the dominant polymorph, accompanied by trace amounts of vaterite. Previous studies [16,17] also reported that the addition of small amounts of ethanol or glycerol as organic additives can facilitate calcite formation during $CaCO_3$ synthesis. The morphologies of the $CaCO_3$ crystals varied noticeably under different additive conditions. Compared with the additive-free sample, the crystals

prepared with organic additives were more fully developed, and their particle sizes were slightly reduced. In the presence of aspartic acid, the crystals were mainly spherical, with a small fraction of dumbbell-shaped particles. With glutamic acid, the crystals were predominantly quasi-spherical. In the ethanol-containing system, the crystals consisted of spherical particles, fine loose aggregates, and a small amount of cubic particles. In the glycerol-containing system, the crystals were mainly spherical.

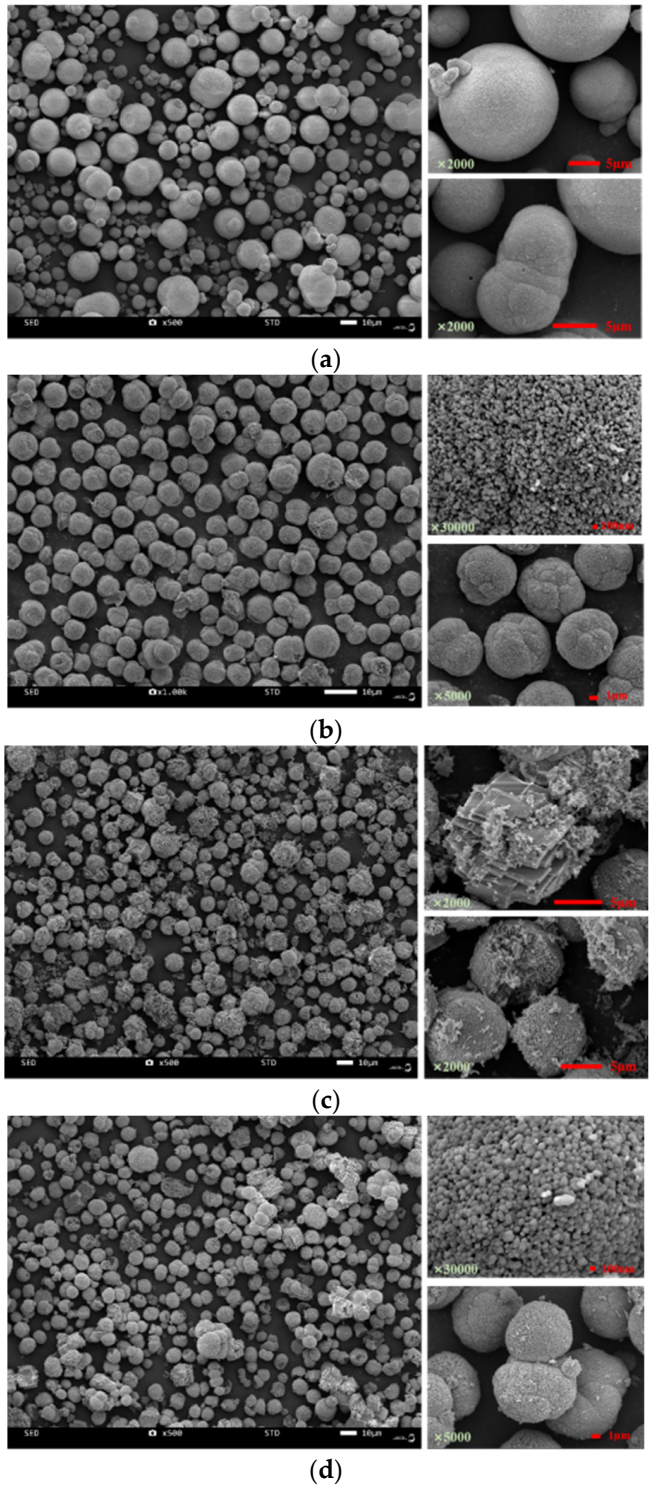

Figure 8. SEM images of $CaCO_3$ synthesized with different organic additives: (**a**) 1 vol% aspartic acid, (**b**) 1 vol% glutamic acid, (**c**) 5 vol% ethanol, and (**d**) 3 vol% glycerol.

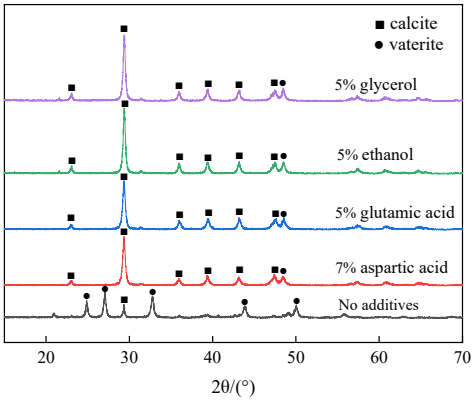

Figure 9. XRD patterns of calcium carbonate with different organic additives.

After dissociation in solution, the negatively charged carboxylate groups of aspartic acid and glutamic acid can bind with Ca^{2+}, thereby providing active sites for $CaCO_3$ crystallization [32]. This interaction may lower the nucleation barrier of metastable vaterite and promote its formation. Owing to its crystal structure, vaterite tends to grow relatively uniformly in different directions, which favors the formation of spherical particles. In addition, amino acid molecules adsorbed on the surfaces of $CaCO_3$ crystallites may impart a negative surface charge, enhancing electrostatic repulsion and weakening van der Waals attraction between particles [33]. As a result, well-dispersed spherical or quasi-spherical $CaCO_3$ particles were obtained. Aspartic acid and glutamic acid can also selectively adsorb onto specific facets of thermodynamically stable calcite [20,21], thereby inhibiting the preferential growth of calcite. This may explain the presence of weak vaterite peaks in the XRD patterns. However, the carbonation process was followed by continuous stirring of the slurry for 2 h before vacuum filtration, during which dissolution and recrystallization may occur [34]. As aspartic acid and glutamic acid complex with dissolved Ca^{2+}, the local ionic activity product may decrease, which can facilitate the transformation of metastable vaterite into thermodynamically stable calcite. This explains why calcite became the dominant phase in the final products.

Ethanol and glycerol can reduce the surface tension of the solution, and their hydroxyl groups may interact with or adsorb onto $CaCO_3$ crystal surfaces. These effects can inhibit anisotropic growth and promote the simultaneous development of multiple crystal faces, resulting in smaller particles and the formation of fine, loose $CaCO_3$ aggregates on the surfaces of spherical particles. Moreover, the addition of ethanol and glycerol increases the solution viscosity, which reduces interparticle collisions and slows Ostwald ripening [16,18]. This further suppresses excessive crystal growth and agglomeration, thereby improving the dispersion of $CaCO_3$ particles. In addition, the hydroxyl groups of ethanol and glycerol may preferentially adsorb onto calcite facets [35,36]. This can stabilize calcite nuclei and inhibit vaterite growth, explaining the dominant calcite diffraction peaks observed in the XRD patterns.

In summary, the addition of all four organic additives led to a slight decrease in particle size, more complete crystal development, and a polymorphic transformation from vaterite to calcite. Among the additives tested, glutamic acid and glycerol showed stronger effects on crystal morphology regulation.

4. Conclusions

(1) The optimized process for preparing $CaCO_3$ from PG by high-pressure carbonation was as follows. PG was first leached for 60 min at 25 °C using 1.5 mol/L NH_4Cl with a liquid-to-solid mass ratio of 60:1, achieving a Ca^{2+} leaching rate of 81.25%. The

resulting Ca^{2+}-rich leachate was then carbonated for 10 min at 25 °C, a CO_2 pressure of 1.0 MPa, and 12 vol% $NH_3 \cdot H_2O$ addition, resulting in a Ca^{2+} conversion rate of 97.36%. The obtained $CaCO_3$ crystals were predominantly vaterite with a quasi-spherical morphology, although particle agglomeration was observed.

(2) High-pressure carbonation was further performed using Ca^{2+}-rich leachates containing organic additives, including aspartic acid, glutamic acid, ethanol, and glycerol. In all additive systems, the Ca^{2+} conversion rate initially increased and then decreased with increasing additive concentration. The optimal dosages were 1 wt% for both aspartic acid and glutamic acid, 5 vol% for ethanol, and 3 vol% for glycerol. The resulting $CaCO_3$ products were predominantly calcite with quasi-spherical morphologies. The particles exhibited relatively uniform sizes and good dispersion. Among the tested additives, glutamic acid and glycerol showed stronger effects on crystal morphology regulation.

Author Contributions: Conceptualization, D.L. and S.H.; methodology, S.H.; validation, D.L., S.H. and X.Z.; formal analysis, S.H.; investigation, S.H.; resources, D.L. and T.Z.; data curation, S.H.; writing—original draft preparation, S.H.; writing—review and editing, T.Z.; visualization, S.H.; supervision, D.L.; project administration, D.L. All authors have read and agreed to the published version of the manuscript.

Funding: This research received no external funding.

Institutional Review Board Statement: Not applicable.

Informed Consent Statement: Not applicable.

Data Availability Statement: The original contributions presented in this study are included in the article. Further inquiries can be directed to the corresponding author.

Conflicts of Interest: Author Taotao Zhang was employed by the company China Nuclear Industry Huaxing Construction Co., Nanjing, China. The remaining authors declare that the research was conducted in the absence of any commercial or financial relationships that could be construed as a potential conflict of interest.

References

1. Pan, Z.W.; Chen, Y.L.; Wu, J.; Tan, Y.Z. Study on the Behavior of Swelling-Shrinkage in Hydration Process of Phosphogypsum-based Super-Sulfated Cement. *J. China Three Gorges Univ. Nat. Sci.* **2023**, *45*, 63–69. [CrossRef]
2. Wang, Q.H.; Wang, C.W.; Huang, Z.Y. Optimization of phosphogypsum allocation for filling based on full-region supply and demand matching: A case study of Yichang City. *J. Saf. Environ.* **2025**, *25*, 1134–1142. [CrossRef]
3. Han, Y.; Lin, R.; Wang, X.Y. Carbon conversion technology for performance improvement and environmental benefits of ultra-high-performance concrete containing slag. *J. Mater. Res. Technol.* **2022**, *21*, 2571–2583. [CrossRef]
4. Wang, C.Q.; Wang, Z.Y.; Huang, D.M.; Huang, C.Q.; Chen, Y. Recovery and recycling core of phosphogypsum: Characteristic hazardous elements risk assessment and analysis. *Process Saf. Environ. Prot.* **2023**, *170*, 738–756. [CrossRef]
5. Zhao, D.; Williams, J.M.; Hou, P.K.; Moment, A.J.; Kawashima, S.H. Stabilizing mechanisms of metastable vaterite in cement systems. *Cem. Concr. Res.* **2024**, *178*, 107441. [CrossRef]
6. Martin, J.B. Carbonate minerals in the global carbon cycle. *Cem. Concr. Res.* **2017**, *449*, 58–72. [CrossRef]
7. Pimentel, C.; Montes-Hernandez, G.; Almarza-Cifuentes, P.; Kellermeier, M.; Van, D.; Alexander, E.S. From Waste to Value: Conversion of Calcium Sulfate to Vaterite via Carbon Capture and Storage. *Adv. Funct. Mater.* **2026**, *36*, e19977. [CrossRef]
8. Wu, Y.N.; Hua, Q.X.; Tang, J.W.; Liu, Y. Studieson preparation technology of calcium carbonate whiskers from phosphogypsum. *Ind. Miner. Process.* **2011**, *40*, 18–22. [CrossRef]
9. Bouargane, B.; Biyoune, M.G.; Mabrouk, A.; Bachar, A.; Bakiz, B. Experimental Investigation of the Effects of Synthesis Parameters on the Precipitation of Calcium Carbonate and Portlandite from Moroccan Phosphogypsum and Pure Gypsum Using Carbonation Route. *Waste Biomass Valorization* **2020**, *11*, 6953–6965. [CrossRef]
10. Hou, J.J.; Liu, Z.D.; Ni, X.Y. Unlocking the mysteries: Investigating the kinetic mechanism of calcium carbonate formation from phosphogypsum. *Process Saf. Environ. Prot.* **2024**, *182*, 625–637. [CrossRef]

11. Altiner, M.; Top, S.; Kaymakoglu, B. Ultrasonic-assisted production of precipitated calcium carbonate particles from desulfurization gypsum. *Ultrason. Sonochem.* **2021**, *72*, 105421. [CrossRef] [PubMed]
12. Lin, Y.; Yan, B.J.; Mitas, B.; Li, C.L.; Fabritius, T. Calcium carbonate synthesis from Kambara reactor desulphurization slag via indirect carbonation for CO_2 capture and utilization. *J. Environ. Manag.* **2024**, *351*, 119773. [CrossRef] [PubMed]
13. Qiao, J.Y.; Chen, Q.J.; Liu, Z.Q.; Ding, W.J. Experimental study on preparation of vaterite-based calcium carbonate by CO_2 mineralization with phosphogypsum. *Ind. Miner. Process.* **2023**, *52*, 14–18, 25. [CrossRef]
14. Chen, Q.G.; Wang, J.; Zhang, Z.Y.; Wang, X.L.; Yang, L. Effects of impurities in leaching liquid of phosphogypsum desulfurization slag on crystal form of calcium carbonate. *Chem. Ind. Eng. Prog.* **2016**, *35*, 3714–3719. [CrossRef]
15. Lopez-Periago, A.M.; Pacciani, R.; Garcia-Gonzalez, C.; Vega, L.F.; Domingo, C. A breakthrough technique for the preparation of high-yield precipitated calcium carbonate. *J. Supercrit. Fluids* **2010**, *52*, 298–305. [CrossRef]
16. Seo, K.S.; Han, C.; Wee, J.H.; Park, J.K.; Ahn, J.W. Synthesis of calcium carbonate in a pure ethanol and aqueous ethanol solution as thesolvent. *J. Cryst. Growth.* **2005**, *276*, 680–687. [CrossRef]
17. Jin, T.T.; Tian, X.L.; Hong, H.L.; Zhu, N.; Han, L.M. Study on preparation and crystalline transformation of nano- and micro-$CaCO_3$ by supercritical carbon dioxide. *Powder Technol.* **2020**, *370*, 29–38. [CrossRef]
18. Konopacka-Lyskawa, D.; Koscielska, B.; Karczewski, J. Effect of some organic solvent-water mixtures composition on precipitated calcium carbonate in carbonation process. *J. Cryst. Growth.* **2015**, *418*, 25–31. [CrossRef]
19. Luo, J.; Kong, F.T.; Ma, X.S. Effects of aspartic acid on polymorph and morphology of calcium carbonate in biomimetic carbonation. *Inorg. Chem. Ind.* **2017**, *49*, 26–30.
20. Yang, S.L.; Gao, Q.; Wang, H.T. Biomimetic mineralization of calcium carbonate with acidic amino acid. *J. Nat. Sci. Heilongjiang Univ.* **2010**, *27*, 495–499+503. [CrossRef]
21. Zhao, Y.Y.; Han, Z.Z.; Yan, H.X.; Zhao, H.; Tucker, M.E. Selective Adsorption of Amino Acids in Crystals of Monohydrocalcite Induced by the Facultative Anaerobic *Enterobacter ludwigii* SYB1. *Front. Microbiol.* **2021**, *12*, 696557. [CrossRef] [PubMed]
22. Zhao, H.P.; Chen, J.; Liu, C.Q.; Wei, S.; Chao, C. Solubility of Calcium Carbonate in Ammonium Chloride Aqueous Solution at T = (298.15, 323.15, and 348.15) K. *J. Chem. Eng. Data.* **2015**, *60*, 3201–3208. [CrossRef]
23. Shen, L.; Sippola, H.; Li, X.; Lindberg, D.; Taskinen, P. Thermodynamic Modeling of Calcium Sulfate Hydrates in the $CaSO_4$–H_2O System from 273.15 to 473.15 K with Extension to 548.15 K. *J. Chem. Eng. Data.* **2019**, *64*, 2697–2709. [CrossRef] [PubMed]
24. Xiao, Y.; Sun, W.J.; Tan, Y.Z.; Sun, D.A.; Xing, D.L. Enhancement of phosphogypsum-based solid waste cementitious materials via seawater and metakaolin synergy: Strength, microstructure, and environmental benefits. *Sustain. Mater. Technol.* **2024**, *41*, e01029. [CrossRef]
25. El-Sheikh, S.M.; Barhoum, A.; Deng, Y. Effects of cationic surfactant during the precipitation of calcium carbonate nano-particles on their size, morphology, and other characteristics. *Colloids Surf. A* **2013**, *422*, 44–49. [CrossRef]
26. Konopacka-Lyskawa, D.; Koscielska, B.; Karczewski, J.; Gołąbiewska, A. The influence of ammonia and selected amines on the characteristics of calcium carbonate precipitated from calcium chloride solutions via carbonation. *Mater. Chem. Phys.* **2017**, *193*, 13–18. [CrossRef]
27. Hu, M.Y.; Huang, M.P.; Jin, S.M.; Guo, Y.H. Technical Process for Synthesis of Vaterite Calcium Carbonate by Using L-aspartic Acid. *Min. Metall. Eng.* **2019**, *39*, 93–96, 101.
28. Wu, L.N.; Chen, X.; Zhang, G.L.; Yang, W.X.; Wu, Q.H. Mineralization and morphology control of $CaCO_3$ induced by glutamic acid derivatized carbon dots. *J. Cryst. Growth.* **2023**, *618*, 127330. [CrossRef]
29. Trushina, D.B.; Bukreeva, T.V.; Kovalchuk, M.V.; Antipina, M.N. $CaCO_3$ vaterite microparticles for biomedical and personal careapplications. *Mater. Sci. Eng. C* **2014**, *45*, 644–658. [CrossRef] [PubMed]
30. Svenskaya, Y.L.; Fattah, H.; Inozemtseva, O.A.; Ivanova, A.G.; Shtykov, S.N. Key Parameters for Size- and Shape-Controlled Synthesis of Vaterite Particles. *Cryst. Growth Des.* **2018**, *18*, 331–337. [CrossRef]
31. Trushina, D.B.; Bukreeva, T.V.; Antipina, M.N. Size-Controlled Synthesis of Vaterite Calcium Carbonate by the Mixing Method: Aiming for Nanosized Particles. *Cryst. Growth Des.* **2016**, *16*, 1311–1319. [CrossRef]
32. Kim, I.W.; Robertson, R.E.; Zand, R. Effects of some nonionic polymeric additives on the crystallization of calcium carbonate. *Cryst. Growth Des.* **2005**, *5*, 513–522. [CrossRef]
33. Deguchi, K.; Osanai, S.C.; Umezawa, S. Synthesis and Physicochemical Properties of Dipeptide Type Surfactants: IN-Dodecanoylglutamyl-glutamic acid and glutamyl-aspartic acid. *J. Oleo Sci.* **2001**, *50*, 763–772. [CrossRef]
34. Luo, M.Z.; Zhang, G.Q.; Fang, Y.H.; Cao, L.Z.; Guo, Z.B. Calcium carbonate crystallization process from the mineralization of calcium chloride waste. *Sep. Purif. Technol.* **2023**, *319*, 124066. [CrossRef]
35. Mokkath, J.H. Impact of Adsorption of Straight Chain Alcohol Molecules on the Optical Properties of Calcite (10.4) Surface. *Nanomaterials* **2022**, *12*, 1460. [CrossRef] [PubMed]
36. Olsen, R.; Leirvik, K.N.; Kvamme, B. Adsorption characteristics of glycols on calcite and hematite. *AIChE J.* **2019**, *65*, e16728. [CrossRef]

Disclaimer/Publisher's Note: The statements, opinions and data contained in all publications are solely those of the individual author(s) and contributor(s) and not of MDPI and/or the editor(s). MDPI and/or the editor(s) disclaim responsibility for any injury to people or property resulting from any ideas, methods, instructions or products referred to in the content.